

Research Paper

Photoactive Poly(3-hexylthiophene) Nanoweb for Optoelectrical Stimulation to Enhance Neurogenesis of Human Stem Cells

Kisuk Yang^{1*}, Jin Young Oh^{2*†}, Jong Seung Lee¹, Yoonhee Jin¹, Gyeong-Eon Chang¹, Soo Sang Chae^{2#}, Eunji Cheong¹, Hong Koo Baik^{2✉}, and Seung-Woo Cho^{1,3✉}

1. Department of Biotechnology, Yonsei University, Seoul 03722, Republic of Korea;
2. Department of Materials Science and Engineering, Yonsei University, Seoul 03722, Republic of Korea;
3. Center for Nanomedicine, Institute for Basic Science (IBS), Seoul 03722, Republic of Korea.

[#]Present address: Department of Chemical Engineering, Stanford University, California 94305, USA.

[†]Present address: Division of Advanced Materials, Korea Research Institute of Chemical Technology (KRICT), Daejeon 34114, Republic of Korea.

*These authors contributed equally to this work.

✉ Corresponding authors: Prof. Seung-Woo Cho, Department of Biotechnology, College of Life Science and Biotechnology, Yonsei University, 50 Yonsei-ro, Seodaemun-gu, Seoul 03722, Republic of Korea; E-mail: seungwoocho@yonsei.ac.kr and Prof. Hong Koo Baik, Department of Materials Science and Engineering, Yonsei University, 50 Yonsei-ro, Seodaemun-gu, Seoul 03722, Republic of Korea; E-mail: thinfilm@yonsei.ac.kr

© Ivyspring International Publisher. This is an open access article distributed under the terms of the Creative Commons Attribution (CC BY-NC) license (<https://creativecommons.org/licenses/by-nc/4.0/>). See <http://ivyspring.com/terms> for full terms and conditions.

Received: 2017.03.20; Accepted: 2017.09.15; Published: 2017.10.13

Abstract

Optoelectrical manipulation has recently gained attention for cellular engineering; however, few material platforms can be used to efficiently regulate stem cell behaviors via optoelectrical stimulation. In this study, we developed nanoweb substrates composed of photoactive polymer poly(3-hexylthiophene) (P3HT) to enhance the neurogenesis of human fetal neural stem cells (hfNSCs) through photo-induced electrical stimulation.

Methods: The photoactive nanoweb substrates were fabricated by self-assembled one-dimensional (1D) P3HT nanostructures (nanofibrils and nanorods). The hfNSCs cultured on the P3HT nanoweb substrates were optically stimulated with a green light (539 nm) and then differentiation of hfNSCs on the substrates with light stimulation was examined. The utility of the nanoweb substrates for optogenetic application was tested with photo-responsive hfNSCs engineered by polymer nanoparticle-mediated transfection of an engineered chimeric opsin variant (CIVI)-encoding gene.

Results: The nanoweb substrates provided not only topographical stimulation for activating focal adhesion signaling of hfNSCs, but also generated optoelectrical stimulation via photochemical and charge-transfer reactions upon exposure to 539 nm wavelength light, leading to significantly enhanced neuronal differentiation of hfNSCs. The optoelectrically stimulated hfNSCs exhibited mature neuronal phenotypes with highly extended neurite formation and functional neuron-like electrophysiological features of sodium currents and action potentials. Optoelectrical stimulation with 539 nm light simultaneously activated both CIVI-modified hfNSCs and nanoweb substrates, which upregulated the expression and activation of voltage-gated ion channels in hfNSCs and further increased the effect of photoactive substrates on neuronal differentiation of hfNSCs.

Conclusion: The photoactive nanoweb substrates developed in this study may serve as platforms for producing stem cell therapeutics with enhanced neurogenesis and neuromodulation via optoelectrical control of stem cells.

Key words: Photoactive nanoweb substrate, Human fetal neural stem cell, Optoelectrical stimulation, Topographical stimulation, Neurogenesis

Introduction

Bioelectrical cues play an important role in the development, maturation, and biological functions of

the nervous system [1, 2]. To employ the beneficial effects of electrical cues for stem cell neurogenesis,

several studies have developed polymer substrates and scaffolds functionalized with various electroconductive materials, thus providing cultured stem cells with electrical stimulation [3-6]. Modification of polymer substrates and scaffolds with electrically conducting polymers (e.g., polyaniline, poly(3,4-ethylenedioxythiophene), polypyrrole) and nanomaterials (e.g., carbon nanotube, graphene) dramatically enhanced the neuronal differentiation of stem cells, as confirmed by upregulated expression of neuronal markers and increased neurite formation and extension [3, 7-13]. Despite promising results from these strategies in promoting neurogenesis, functionalization of polymeric systems by incorporation of electroconductive polymers and nanomaterials often damages and denatures the polymeric substrates and scaffolds, as well as causes significant cytotoxicity, reducing the potential utility of such methods for biomedical engineering applications. Thus, alternative strategies to circumvent these problems must be established to develop biocompatible, electrically active polymeric systems capable of generating electrical cues for enhanced neurogenesis of stem cells.

Optoelectrical stimulation that converts light into an electrical signal can overcome the limitations of current strategies relying on electroconductive moiety modification by providing a highly biocompatible and effective method of producing electrical cues for stem cell neurogenesis [14]. Recently, optoelectrical signals have been examined for stimulating living cells and efficiently manipulating cellular behaviors [15]. Organic photovoltaics capable of converting light energy into electrical power, which have been successfully utilized as environment-friendly solar cells in energy fields, may provide stem cells with optoelectrical stimulation upon light exposure at the proper wavelength. Because this strategy employs light-induced electrical power, it can produce electrical cues for modulating stem cell behaviors without any harmful byproducts or direct damage to cells. Among several organic photovoltaics, poly(3-hexylthiophene) (P3HT) shows promise as a photoactive polymeric platform for stem cell neurogenesis. P3HT has been applied as a representative photoactive polymer for solar cells and photo-sensors in organic electronics because of its ability to efficiently produce electricity by absorbing most visible light. P3HT-based organic photovoltaics have also been used as wireless electrical supply units for tissue-engineering applications [16]. More recently, this platform was applied for electrical stimulation under illumination with near-infrared light to promote the differentiation and neurite

outgrowth of PC12 cells [15]. P3HT has also shown excellent biocompatibility in several studies with primary cells. As one of such examples, photosensitive polymer scaffolds with incorporation of P3HT and epidermal growth factor significantly improved proliferation of skin fibroblasts and epidermal differentiation of stem cells under light stimulation [17]. P3HT-based hybrid bioorganic interface was also reported for photoactivation of primary neurons, where action potentials in neurons could be triggered with short pulses of visible light stimulation [18].

P3HT can be engineered to achieve better performance to improve the neurogenesis of stem cells. P3HT is easily transformed into one-dimensional (1D) nanostructures (nanoweb) such as nanofibrils (NFs) or nanorods (NRs) via self-assembly of polymer molecules in solution and the formed nanostructures can be controlled by regioregularity of polymer or solvent properties [19-21]. The nanoweb film consisting of crystalline P3HT-NF and P3HT-NR showed improved electrical and optical properties because of its extremely large surface area with good electrical interconnectivity between 1D nanostructures compared to two-dimensional (2D) film, thus enhancing the photocurrent in bulk-heterojunction and bilayer organic solar cells [19, 22]. Moreover, the P3HT nanoweb with NF and NR structures can provide topographical stimulation to manipulate diverse stem cell behaviors including adhesion, proliferation, and differentiation. Topographical cues have been reported to affect integrin clustering, focal adhesion, and actin remodeling, ultimately altering mechanosensitive signaling cascades involved in stem cell differentiation [23-26]. Therefore, these features of photoactive P3HT nanoweb can significantly contribute to the promotion of stem cell neurogenesis by simultaneously providing the stem cells with light-induced electrical stimulation and topographical stimulation. Interestingly, photoactive polymer photovoltaics may also be useful for optogenetics, a promising biological technique that uses light to regulate the behaviors of cells or tissues [27]. Because light exposure can stimulate both modified cells to overexpress light-sensitive ion channels and polymer photovoltaics simultaneously, optoelectrical stimulation can be synergistically increased, thus enhancing highly mature neuronal phenotypic differentiation and functional maturation of optogenetically modified stem cells on the P3HT nanoweb.

In this study, we developed optoelectrical P3HT nanoweb platforms to promote the neurogenesis of human fetal neural stem cells (hfNSCs). Optoelectrical

stimulation of hfNSCs grown on a photoactive P3HT nanoweb with NF or NR structures not only induced activation of focal adhesion signaling, but also facilitated neuronal differentiation and electrophysiological maturation of hfNSCs. hfNSCs on bare glass or planar P3HT substrates did not exhibit such improvements in neurogenesis. Interestingly, optoelectrical stimulation of optogenetically modified hfNSCs on the P3HT nanoweb substrates further promoted hfNSC neurogenesis by upregulating the expression and activation of ion channels, suggesting the novel concept of single external stimuli-mediated simultaneous activation of multiple components (e.g., photo-responsive cells and photoactive polymer substrates) in neural tissue engineering. Our study suggests the utility of optoelectrical polymer nanostructured substrates to produce neuronal cells exhibiting functionally matured neuronal phenotypes from human stem cells. In addition, our system may be a key technology for the development of photo-responsive wireless and implantable bioelectronics for promoting neurogenesis.

Materials and Methods

Fabrication and Characterization of Poly(3-hexylthiophene) (P3HT) Nanoweb Substrates

The P3HT substrates were prepared as reported previously [22]. Briefly, nanofibril (NF) or nanorod (NR) of P3HT purchased from Reike Metal Inc. (Lincoln, NE, USA) (regioregularity ~95%, ~98% and $M_w = 50,000$) was formed by a cycle of cooling (-20°C) and heating (room temperature) in P3HT solution (0.25 wt%, *m*-xylene). The P3HT solution was spin-coated onto the glass substrate. The P3HT film (30 nm in thickness) was then dried at 100°C for 10 min in a glove box. For surface characterization, the topography of the fabricated P3HT nanoweb substrates was observed by scanning electron microscopy (SEM; FEI Sirion SEM, Hillsboro, OR, USA) [28]. Optical analyses were performed by UV-vis spectroscopy (V-570, Jasco Inc., Easton, MD, USA) and photoluminescence spectroscopy (LS55, Perkin Elmer Inc., Waltham, MA, USA). The photovoltaic devices (I-V characteristic) were characterized using a Keithley 236 source meter (Keithley Instruments, Cleveland, OH, USA) under a green light-emitting diode (LED) light.

Human Fetal Neural Stem Cell (hfNSC) Culture

The expansion of hfNSCs in a self-renewal state was carried out according to our previous study [23].

The P3HT substrates were coated with fibronectin (FN) by a simple dip-coating method in a $10\ \mu\text{g}/\text{mL}$ FN solution (Sigma, St. Louis, MO, USA) for 2 h. For spontaneous differentiation, hfNSCs dissociated from the neurospheres were seeded onto the P3HT substrates at a seeding density of 4.5×10^4 cells/ cm^2 and maintained under Dulbecco's Modified Eagle Medium: Nutrient Mixture F-12 (Gibco, Grand Island, NY, USA) medium without mitogenic factors (fibroblast growth factor (bFGF) and leukemia inhibitory factor (LIF), Sigma) according to our previous protocol [29].

Optoelectrical Stimulation

Starting one day after hfNSC seeding onto P3HT substrates, the cells were optically stimulated with a green light (539 nm) using a LED (maximum current: 20 mA, maximum voltage: 3.4 V). Pulsed optoelectrical stimulation (pulse duration 1 s, 1 Hz, 30 min twice per day) was applied to hfNSCs on the P3HT substrates to produce optimal electrical parameters for neuronal cell culture and differentiation [15]. The light intensity of the green LED was $7\ \text{mW}/\text{cm}^2$. The position of the LED was fixed above the well plate containing P3HT substrate in each well and the distance between the P3HT substrate and the LED was set to be 2.5 cm. After 7 days in culture, the expression of neuronal markers (Neuronal class III β -tubulin (Tuj1) and Microtubule-associated protein 2 (MAP2)) and ion channels (voltage-gated sodium channel alpha subunit 1 (SCN1 α) and L type, calcium channel alpha 1C subunit (CACNA1C)) in hfNSCs was quantified by quantitative real-time polymerase chain reaction (qPCR) analysis.

Live/Dead Staining

After 2 days of culture, the viability of hfNSCs was examined by staining the cells with the Live/Dead assay kit (Invitrogen, Carlsbad, CA, USA) according to our previously described protocol [30]. The cells were exposed to green light the next day after cell seeding and the viability test was performed one day later. The cells on glass substrates without light exposure served as a control group.

Immunocytochemistry

Immunocytochemical staining was conducted according to our previously described protocol [31]. The following primary antibodies were used for staining: mouse monoclonal anti-Tuj1 (1:100; Millipore, Billerica, MA, USA), rabbit polyclonal anti-MAP2 (1:200; Santa Cruz Biotechnology, Santa Cruz, CA, USA), rabbit polyclonal anti-gial fibrillary acidic protein (GFAP) (1:200; Millipore), mouse

monoclonal anti-glutamic acid decarboxylase (GAD67) (1:200; Abcam, Cambridge, UK), rabbit polyclonal anti-glutamate transporter (GluT) (1:200; Abcam), and rabbit polyclonal anti-neurofilament 200 (NF200) (1:200; Sigma). The following secondary antibodies were used: Alexa Fluor-488 goat anti-mouse IgG (1:500) and Alexa Fluor-488 donkey anti-rabbit IgG (1:500) (Invitrogen). Cell nuclei were counterstained with 4',6-diamidino-2-phenylindole (DAPI, Sigma). The fluorescently stained signals were detected under a confocal microscope (LSM 700, Carl Zeiss, Jena, Germany). Neurite formation and cell body length were quantified from Tuj1- or MAP2-stained cell images as described in our previous study [24]. Focal adhesion staining (vinculin) was performed using the FAK100 kit (Millipore).

Gene Expression Analysis

qPCR analysis was performed according to our previously described protocol [32]. TaqMan Gene Expression Assays (Applied Biosystems, Foster City, CA, USA) were used to measure the gene expression in hfNSCs on the substrates for each target Tuj1: Hs00801390_s1, MAP2: Hs00258900_m1, SCN1 α : Hs00374696_m1, CACNA1C: Hs00167681_m1, Focal adhesion kinase (FAK): Hs01056457_m1, vinculin: Hs00419715_m1, and glyceraldehyde 3-phosphate dehydrogenase (GAPDH): Hs02758991_g1). The gene expression level in each group was determined by using the comparative C_t method and the expression of each target gene was normalized to that of an endogenous reference transcript (GAPDH) [33].

Western Blotting

Western blotting analysis was performed as described in our previous study [24]. The following primary antibodies were used: rabbit polyclonal anti-FAK (pY397, 1:1000; Invitrogen) and rabbit polyclonal anti- β -actin (1:2000; Cell Signaling Technology, Beverly, MA, USA). Target protein signals were detected with a Clarity Western ECL Substrate (Bio-Rad, Hercules, CA, USA) according to the manufacturer's instructions.

Electrophysiology

Electrophysiological analysis was performed using the protocol described in our previous study [24]. Whole cell patch-clamping for measuring action potential and ion channel current of hfNSCs differentiated on the substrates was performed after 7 days of culture. The cells were treated with tetrodotoxin (TTX) (0.5 μ M) (Sigma) for 5 min to identify whether the currents and spikes were specific to the sodium channel.

Calcium Imaging

For calcium influx imaging, after 7 days of culture, hfNSCs on the P3HT-NF were stained with Fluo-4 AM dye (Invitrogen) before optoelectrical stimulation. Time-lapse changes in calcium influx levels in live hfNSCs were imaged using a confocal microscope (LSM 700, Carl Zeiss) under optoelectrical stimulation (1 Hz).

Transfection

For optogenetic modification of hfNSCs, the cells were transfected with the *Chlamydomonas reinhardtii* Channelrhodopsin-1 (ChR-1) and *Volvox carterii* ChR-1 (C1V1) E122T/E162T (ET-ET)/enhanced yellow fluorescent protein (EYFP) (C1V1 ET-ET/EYFP) plasmids (1 μ g per 10^5 cells, Vector Core Facility, University of North Carolina Chapel Hill, Chapel Hill, NC, USA) by electroporation at 1200 V and 20 ms width (Neon, Invitrogen). The transfected hfNSCs were seeded onto FN-coated P3HT substrates. After 2 days, hfNSCs were transfected once more with the plasmids (5 μ g per 10^5 cells) by using previously optimized conditions with C32-122 poly(β -amino ester) (PBAE) nanoparticles [34].

Statistical Analysis

Statistical analyses were conducted with an unpaired Student's *t* test using Sigma-Plot software (Systat Software Inc., Chicago, IL, USA) as previously described [35]. The values of $p < 0.01$ or 0.05 were considered statistically significant.

Results and Discussion

Fabrication and Characterization of P3HT Substrates

In this study, photoactive nanoweb P3HT substrates were fabricated to generate optoelectrical stimulation for enhanced neurogenesis of hfNSCs. Fig. 1 shows the schematic illustration of the process used to prepare the P3HT nanoweb films with NFs or NRs. Self-assembled P3HT-NR and P3HT-NF were formed with different regioregularities of P3HT through a cycle of cooling and healing processes in solution [19, 20]. P3HT with higher regioregularity formed into relatively shorter length and larger diameter 1D nanostructures than P3HT with lower regioregularity because of the relatively high rigidity of the conjugated polymer backbone (Fig. 1) [20]. SEM analysis showed the surfaces of planar P3HT and nanoweb P3HT films with NFs or NRs (Fig. 2A). All films were spin-coated with different P3HT solutions on glass substrates. The planar P3HT film had a smooth surface, while the P3HT nanoweb films

showed NF or NR structures on the surfaces (Fig. 2A). The NF had a ~ 15 nm diameter and was over $1 \mu\text{m}$ in length. The NR had a larger diameter (~ 25 nm) and shorter length (~ 500 nm) than the NF. The NF web showed a better continuous NF network, while the NR web had a higher packing density of NR [20]. The water contact angles of the planar P3HT, P3HT-NF, and P3HT-NR surfaces were $99.7^\circ \pm 1.0^\circ$, $96.0^\circ \pm 1.5^\circ$, and $91.4^\circ \pm 3.3^\circ$, respectively (Fig. 2B). A FN coating was applied to facilitate hfNSC adhesion, which rendered the surfaces more hydrophilic, as indicated by a significant decrease in the water contact angle ($38.3^\circ \pm 3.3^\circ$, $32.4^\circ \pm 4.4^\circ$, and $36.7^\circ \pm 6.1^\circ$) (Fig. 2B). This level of hydrophilicity is generally suitable for facilitating cellular adhesion [36]. The water contact angle measurement assay also revealed similar surface properties of the planar P3HT film (P3HT) and two P3HT nanoweb substrates (P3HT-NF, P3HT-NR). The water contact angles of the bare glass and FN-coated glass surfaces were $12.1^\circ \pm 1.4^\circ$ and $31.0^\circ \pm 3.3^\circ$, respectively (Fig. 2B).

P3HT nanoweb substrates possess optical properties to efficiently provide the hfNSCs with electrical cues via light-induced excitation. The P3HT absorbs most visible light (400–650 nm) with a main absorption peak at ~ 550 nm, as shown in Fig. 2C, which corresponds to the light wavelength of a green LED (Fig. 2D). The degree of electron transfer from P3HT to the electron acceptor depends on the

interface area between the electron donor (P3HT) and acceptor (stem cells), as the exciton generated by light in P3HT is separated by the interface of the electron donor and acceptor [22]. Thus, photoluminescence (PL) emission of P3HT films with hfNSCs on their surfaces was measured to evaluate electron charge transfer into hfNSCs as electron acceptors, which leads to PL quenching. Fig. 2E shows the PL emission intensity of various types of P3HT layers (30 nm in thickness). The PL emission of planar P3HT films under hfNSCs was quenched to 25.4% and PL emission of the NR and NF-based nanoweb P3HT films was further quenched to 37.7% and 55.6%, respectively (Fig. 2E), indicating that the nanoweb P3HT films, particularly that with NF structures, had a larger surface area and more favorable surface morphology for efficiently transferring electrons to the electron acceptor (hfNSCs) than the planar surface. This advantage of nanoweb P3HT film was further verified with an organic solar cell composed of a bi-layer of an electron donor and acceptor. The current-voltage curves and photovoltaic parameters of the bilayer organic solar cells are shown in Fig. 2F and G. Phenyl-C61-butyric acid methyl ester (PCBM) was applied as a representative electron acceptor in the organic solar cell to evaluate the generation of photocurrent depending on the surface morphology of P3HT film. Upon light exposure, the solar cell with the nanoweb P3HT/PCBM bi-layer showed greater

short-circuit current (J_{sc}), which represents a greater photocurrent and higher power conversion efficiency than the solar cell with the planar P3HT/PCBM bi-layer (Fig. 2F and G), indicating more efficient generation of free charge carriers on the larger surface area of the P3HT nanoweb with a continuous network. Wu *et al.* reported that the up-conversion (UC) effects of UC nanocrystals noticeably enhanced the photocurrent and the efficiency of the organic photovoltaic devices under illumination by monochromatic light (980 nm) [37].

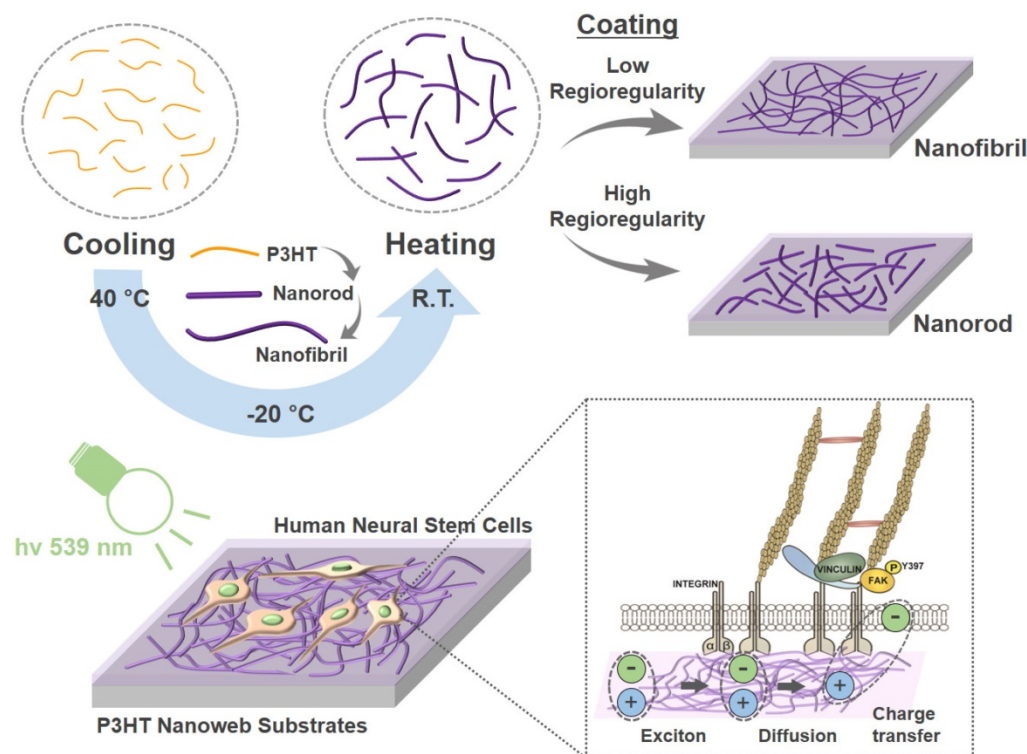


Figure 1. Schematic illustration of fabrication and application of photoelectrical poly(3-hexylthiophene) (P3HT) nanoweb substrates for enhancing neuronal differentiation of human fetal neural stem cells (hfNSCs).

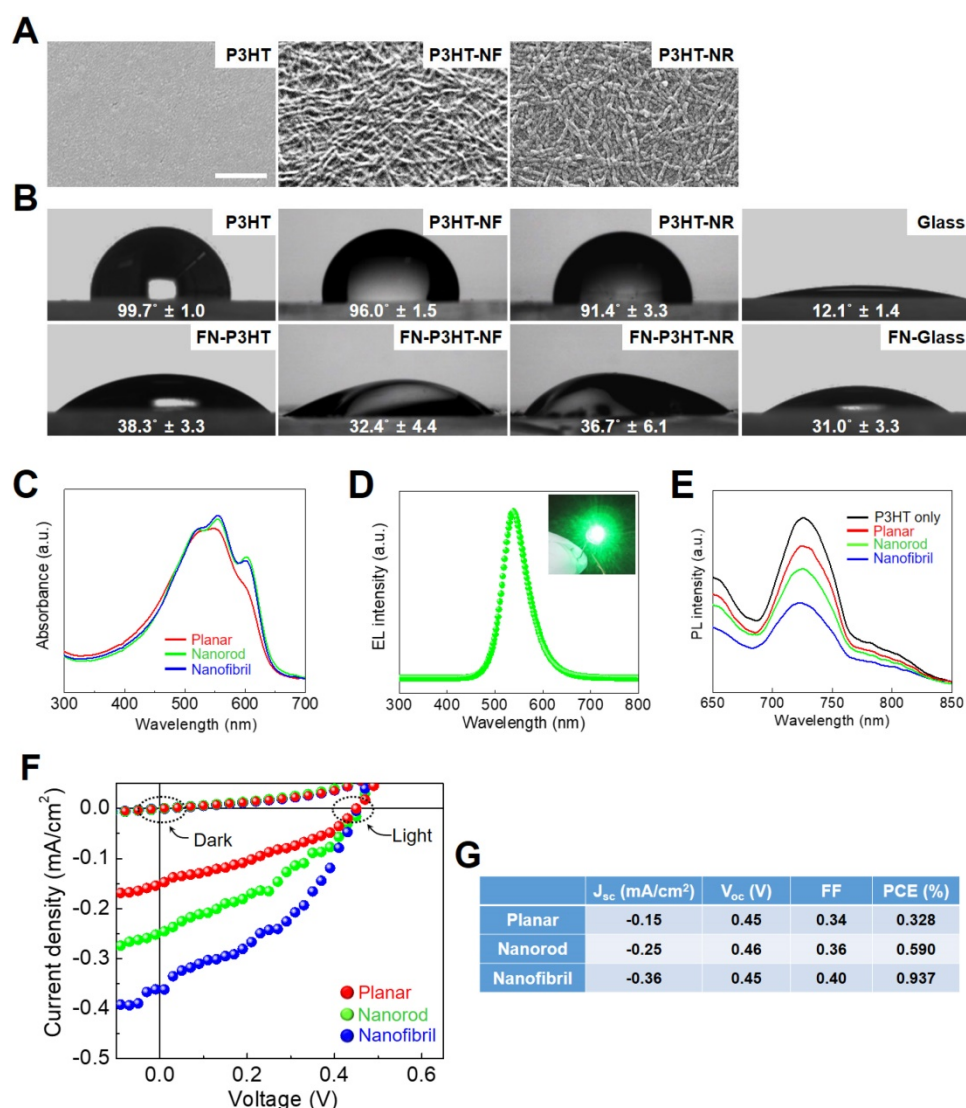


Figure 2. Surface characterization of photoactive nanoweb P3HT substrates. (A) SEM images of P3HT nanoweb substrates with nanofibril (NF) or nanorod (NR), scale bar = 300 nm. (B) Measurement of water contact angle of planar P3HT (P3HT), P3HT nanoweb (P3HT-NF, P3HT-NR), fibronectin (FN)-coated planar P3HT (FN-P3HT), and FN-coated P3HT nanoweb (FN-P3HT-NF, FN-P3HT-NR). (C) UV-vis absorbance spectra of planar and nanoweb (NF or NR) P3HT films. (D) Electroluminescence spectra of green light-emitting diode (LED). (E) Photoluminescence spectra of single P3HT layer (30 nm) and hfNSC/P3HT (30 nm) bi-layer. (F, G) Photovoltaic property of bi-layer (P3HT/PCBM) organic solar cell. (F) I-V curves of organic solar cells composed of various P3HT layers (planar, nanorod, and nanofibril) under green LED light (539 nm). (G) Photovoltaic characteristics calculated from I-V curves. Device structure: ITO/poly(3,4-ethylenedioxythiophene (PEDOT):PSS (40 nm)/P3HT (30 nm)/PCBM (30 nm)/LiF (1 nm)/Al (100 nm).

Enhanced Focal Adhesion Development of hfNSCs by P3HT Nanoweb

The fabricated P3HT nanoweb can provide topographical cues for enhancing the neuronal differentiation of hfNSCs. First, we evaluated the biocompatibility of the P3HT substrates. A live/dead staining assay after 2 days in culture showed highly viable hfNSCs on the P3HT-NF substrates (Fig. S1). The hfNSCs remained viable on the P3HT-NF substrates following optoelectrical stimulation at 539 nm (Fig. S1A). Quantification data of cell viability from live/dead-stained images clearly indicated that the viability of hfNSCs on P3HT-NF substrates was around 90%, similar level to that on glass substrates,

irrespective of light stimulation (Fig. S1B). Based on this result, we could confirm the biosafety of semiconductive P3HT polymer. To evaluate the structural and topographical effects of the P3HT nanoweb on cellular behaviors, we examined whether P3HT substrates with nanoweb structures could expedite focal adhesion development in hfNSCs. It has been demonstrated that topographical cues can regulate diverse cellular behaviors including survival, proliferation, differentiation, and migration [38-43] by modulating focal adhesion and subsequent mechanosensitive signaling cascades [23, 24, 44]. Therefore, topographical features with specific shapes, scales, and dimensions have been applied to regulate stem cell differentiation [23-26]. In this study,

we found that the P3HT with NF structure (P3HT-NF) was more effective for facilitating focal adhesion development in hfNSCs likely by providing more focal adhesion points than glass, planar P3HT (P3HT), or P3HT with an NR structure (P3HT-NR), as indicated by the greatest increase in expression of the focal adhesion protein vinculin (Fig. 3A). SEM observation of hfNSCs on the substrates also indicated that the P3HT nanoweb substrates with NF provided a larger number of adhesion sites for focal adhesion development than other substrates (Fig. 3B). qPCR assay also supported this result by showing that the gene expression of vinculin and FAK was highest in hfNSCs cultured on P3HT-NF substrates compared to in cells cultured on other substrates (Fig. 3C). The structural features of the P3HT-NF nanoweb, which has a continuous network of NF structures with greater length and shorter diameter than P3HT-NR, may be more advantageous for developing focal adhesion in hfNSCs.

The P3HT substrates with NF nanotopography activate the FAK pathway to promote stem cell differentiation. The culture of hfNSCs on P3HT-NF substrates substantially increased the phosphorylation of FAK at Y397 compared to hfNSCs cultured on other substrates such as glass, planar P3HT, and P3HT-NR substrates, as confirmed by western blotting analysis (Fig. 3D). It is known that FAK autophosphorylation at Y397 is induced by integrin clustering and actomyosin contractile tension [45]. Enhanced integrin clustering by nanotopographies can facilitate FAK recruitment and trigger FAK autophosphorylation at Y397, which is required for full activation of FAK [29, 46]. FAK signaling activation affects the maturation of focal adhesion and ultimately controls stem cell differentiation [47, 48]. In our previous study, we confirmed that enhanced integrin clustering and cytoskeletal alignment by topographical cues facilitate FAK recruitment to adhesion sites and phosphorylation of FAK (Y397), contributing to focal adhesion development and neuronal differentiation of hfNSCs [23, 24, 29]. Similarly, our current data show that the topography of P3HT-NF facilitates focal adhesion development and activates FAK-associated signaling pathways in hfNSCs, eventually promoting hfNSC neurogenesis.

Enhancement of Neuronal Differentiation and Functional Maturation of hfNSCs on P3HT Nanoweb Substrates with Optoelectrical Stimulation

Next, we investigated whether optoelectrical stimulation of the P3HT nanoweb substrates could enhance the neuronal differentiation of hfNSCs.

Although numerous studies have examined the interactions of neural stem cell (NSC) differentiation and nanomaterials, few studies have evaluated the biological effects of photoelectrical stimulation on NSC differentiation. Akhavan *et al.* showed that reduced graphene oxide (rGO)-titanium oxide (TiO₂) heterojunction substrates with flash photo-stimulation enhanced the differentiation of NSCs into the neuronal lineage [49]. They demonstrated that neuronal differentiation of NSCs was promoted by electron injection from the photo-excited TiO₂ into cells on the rGO through Ti-C and Ti-O-C bonds. However, because the substrates composed of a mixture of TiO₂ and rGO used in this previous study did not provide specific topographies on the surface, topographical effects cannot be expected for NSC differentiation. In our study, to induce the spontaneous differentiation of hfNSCs, cells on the P3HT substrates with nanoweb structures were maintained under culture conditions without mitogenic factors, bFGF and LIF. Next, green light (539 nm) generated by an LED lamp was applied to the P3HT substrates to provide pulsed optoelectrical stimulation to the hfNSCs (1 Hz, 30 min twice per day). We adapted this protocol for pulsed optoelectrical stimulation because our P3HT substrates with this stimulation protocol produced photovoltaic parameters (P3HT planar; open-circuit voltage (V_{oc}) of 0.45 V, short-circuit current (J_{sc}) of -0.15 mA/cm², and fill factor (FF) of 0.34 in Fig. 2F and G), similar to the values previously confirmed to be appropriate for neural cell culture and differentiation (V_{oc} of 0.42 V, J_{sc} of 0.17 mA/cm², and FF of 0.32) [15]. In our previous study reporting the development of a novel electrical stimulation platform to accelerate direct neuronal conversion and neuronal maturation [34], we optimized electrical stimulation parameters and identified the particular values that do not affect cell viability but significantly increase neuronal transdifferentiation. Actually, photoactivity of P3HT in aqueous solution has already been verified to be similar to its solid state, allowing for diverse applications as a photocatalyst in aqueous solution [50-52]. Although a comprehensive study would be required for further characterization of P3HT photovoltaic devices in cell culture medium, P3HT could be a highly effective photoreactive polymeric materials for organic bioelectronics to enhance stem cell neurogenesis in hfNSC culture system. After 7 days of culture, immunocytochemical analysis was performed to determine the expression of neuronal markers, Tuj1, MAP2, and NF200, in hfNSCs grown on each substrate.

P3HT-NF substrate with pulsed optoelectrical stimulation using 539 nm green light significantly

promoted the neuronal differentiation of hfNSCs compared with other substrates (glass, planar P3HT, and P3HT-NR), as indicated by the larger number of Tuj1- and MAP2-positive cells and more extensive NF200-positive neurite outgrowth (Fig. 4A and Fig. S2). Neurite formation and the length of neurite outgrowth were quantified using Tuj1-stained images because neurite formation is important for communication between neurons and formation of the intricate circuitry of the entire nervous system [53]. Neurite formation and outgrowth were more extensive in the P3HT-NF group than in the other groups, and optoelectrical stimulation of P3HT-NF further promoted neurite formation and outgrowth from hfNSCs (Fig. 4B). Yu-sheng *et al.* also demonstrated that the system with organic photovoltaics and a bioelectronics interface provided direct electrical stimulation using optical sources for promoting neurite formation and manipulating the polarity of neuronal cells [15]. Hsiao *et al.* demonstrated multifunctional organic bioelectronics for manipulating human mesenchymal stem cell (hMSC) differentiation [54]. In these organic

bioelectronics, rGO material was applied as an adhesive coating to promote adhesion and alignment of hMSCs and dexamethasone-loaded poly(3,4-ethylenedioxythiophene) (PEDOT) microelectrode array served as an electroactive drug-releasing electrode to enhance osteogenic differentiation of hMSCs under electrical stimulation. qPCR analysis performed at days 4 and 7 in hfNSC culture revealed that gene expression of the neuronal markers Tuj1 and MAP2 was upregulated in hfNSCs grown on P3HT-NF substrates (Fig. 4C and D). The gene expression of Tuj1 and MAP2 was further increased in hfNSCs on P3HT-NF substrates when activated with optoelectrical stimulation by 539 nm light (Fig. 4C and D). These results indicate that the combined effect of topographical and optoelectrical stimulations of P3HT substrates with NF structures can dramatically promote neuronal differentiation of hfNSCs. This may be because NF structures on P3HT can induce the most efficient photo-induced electron transfer (Fig. 2E–G) and provide the greatest number of focal adhesion points (Fig. 3) compared to planar or NR structures.

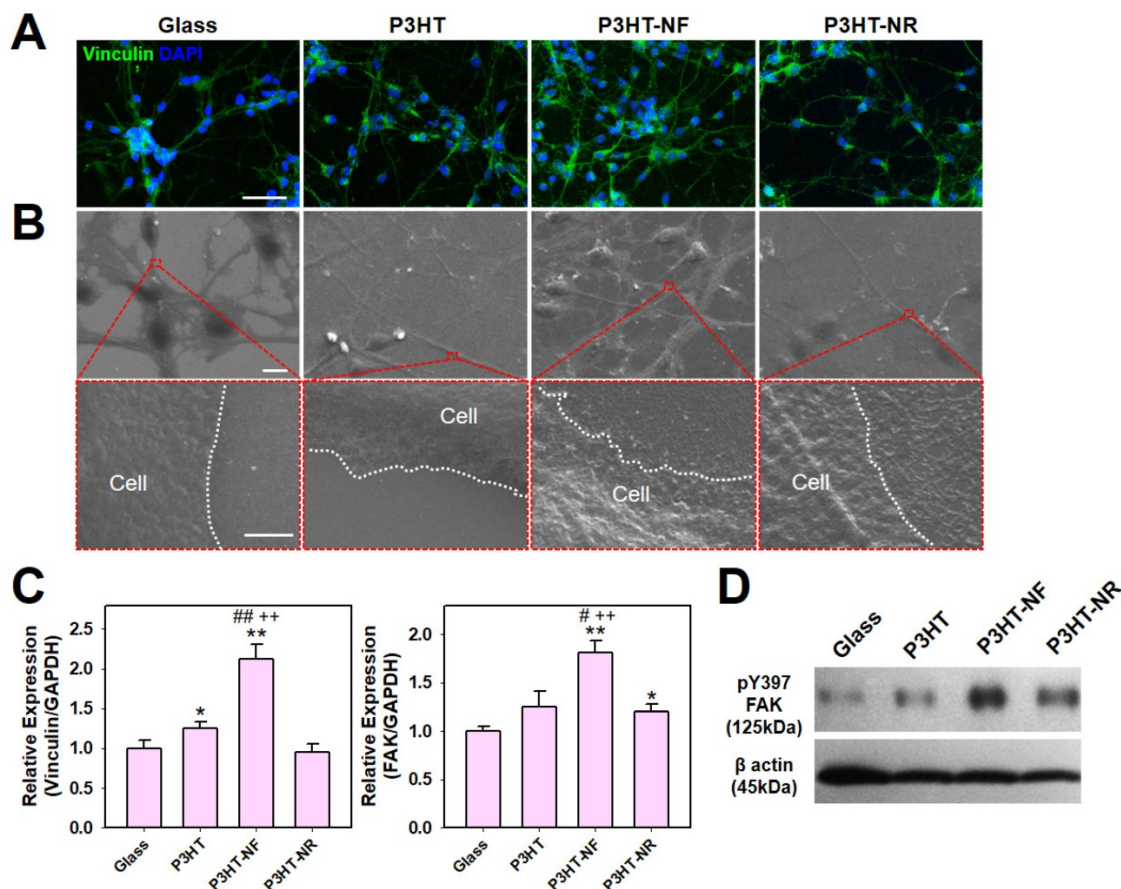


Figure 3. Focal adhesion development of hfNSCs on P3HT substrates after 4 days in culture. (A) Staining of focal adhesion protein vinculin (green) in hfNSCs on glass, planar P3HT, P3HT-NF, and P3HT-NR substrates, scale bar = 50 μm . (B) SEM images of hfNSCs on each substrate (top rows), scale bar = 10 μm . High magnification images of hfNSCs on each substrate (bottom rows), scale bar = 1 μm . (C) qPCR analysis to examine the gene expression of focal adhesion proteins (vinculin and FAK) in hfNSCs grown on each substrate ($n = 3$, *; $p < 0.05$, **; $p < 0.01$, compared to glass group, #; $p < 0.05$, ##; $p < 0.01$, compared to P3HT group, ++; $p < 0.01$, compared to P3HT-NR group). (D) Western blot analysis of phosphorylated FAK [pFAK (Y397)] expression in hfNSCs grown on each substrate. β -actin was used as a loading control for comparison of pFAK (Y397) protein expression.

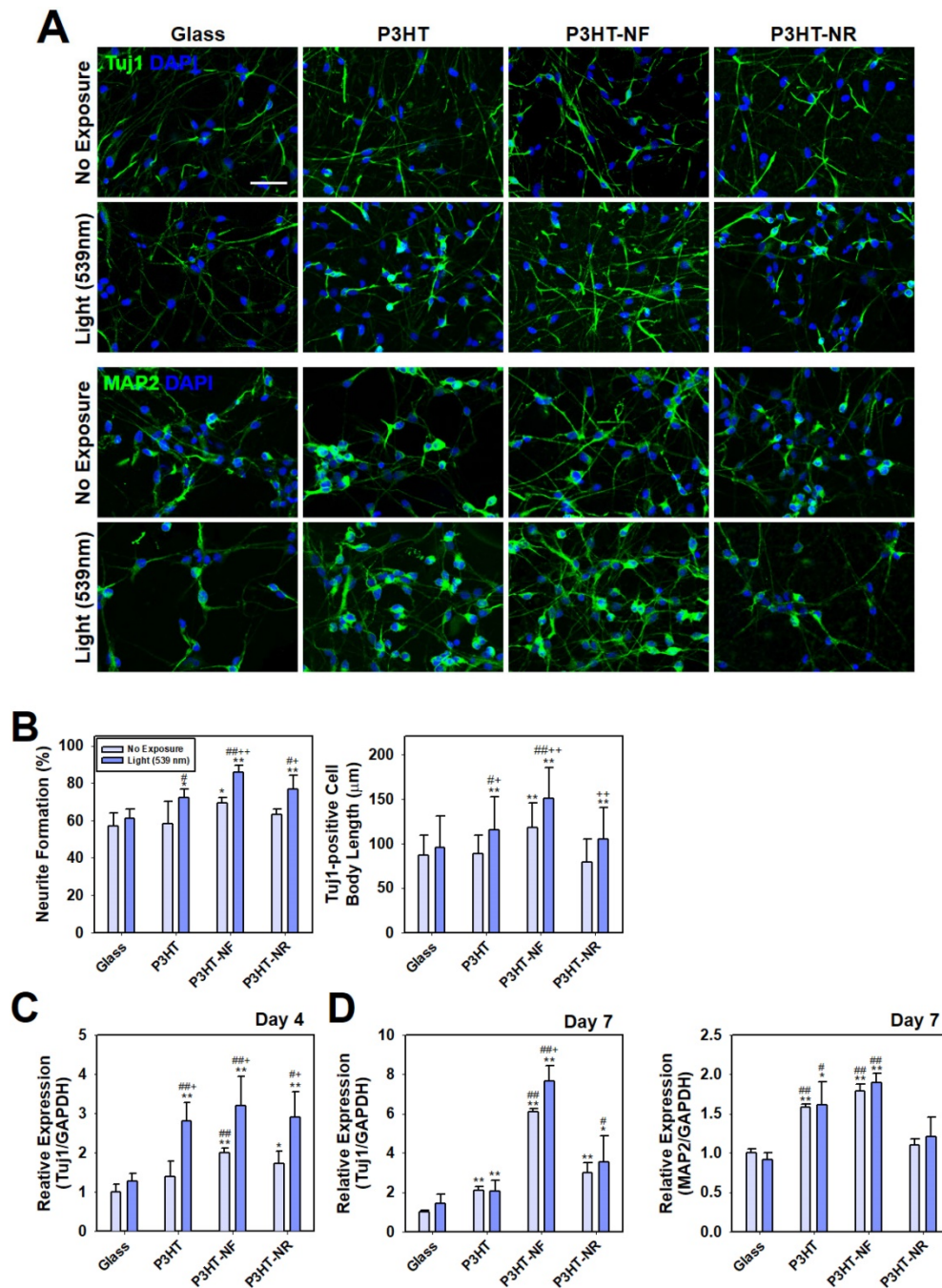


Figure 4. Differentiation of hfNSCs on P3HT substrates after 7 days in culture. (A) Immunofluorescence staining for neuronal markers (Tuj1 and MAP2) of hfNSCs differentiated on each substrate with or without 539 nm light stimulation, scale bar = 50 µm. (B) Quantification of neurite formation ($n = 4$) and the length of neurite outgrowth ($n = 30-50$) in the Tuj1-stained images (*; $p < 0.05$, **; $p < 0.01$, compared to glass without light, #; $p < 0.05$, ##; $p < 0.01$, compared to glass with light, +; $p < 0.05$, ++; $p < 0.01$, compared to each substrate without light). (C, D) qPCR analysis to measure the gene expression of Tuj1 and MAP2 in hfNSCs grown on each substrate after 4 and 7 days of culture (*; $p < 0.05$, **; $p < 0.01$, compared to glass without light, #; $p < 0.05$, ##; $p < 0.01$, compared to glass with light, +; $p < 0.05$, compared to each substrate without light).

To examine the differentiation propensity of hfNSCs into neuronal and astrocytic lineage cells by electrical stimulation, immunofluorescent staining for neuronal marker (Tuj1) and astrocyte marker (GFAP) was performed and quantification data of the population of Tuj1- or GFAP-positive cells in each group was shown in Fig. S3. When light stimulation

was applied to hfNSCs in all groups, the population of Tuj1-positive cells to total cells (DAPI-positive cells) was the highest in the P3HT-NF group ($53.8\% \pm 4.0\%$), compared to other groups (glass group; $40.5\% \pm 5.4\%$, P3HT group; $48.5\% \pm 4.0\%$, P3HT-NR group; $50.0\% \pm 3.2\%$). On the other hand, the population of GFAP-positive cells was the lowest in the P3HT-NF

group ($33.2\% \pm 2.6\%$) compared to other groups (glass group; $39.4\% \pm 2.4\%$, P3HT group; $36.4\% \pm 1.9\%$, P3HT-NR group; $35.0\% \pm 2.0\%$). These data demonstrate that optoelectrical stimulation of hfNSCs on P3HT substrates enhanced neuronal differentiation of the stem cells but did not promote glial lineage differentiation. To check neuronal subtypes of differentiated hfNSCs, we have also conducted immunofluorescent staining for GluT and GAD, and quantified the percentage of GluT- or GAD- positive cells in total cell population (Fig. S4). It was confirmed that the culture of hfNSCs on the P3HT-NF with optoelectrical stimulation facilitates hfNSC differentiation to inhibitory neuronal lineage (e.g., GABAergic neuron; GAD-positive cells) rather than to excitatory neuronal lineage (e.g., glutamatergic neuron; GluT-positive cells).

The efficacy of hfNSC neurogenesis was also compared between our photoelectrical stimulation method (P3HT-NF substrate) and conventional culture (glass substrate) or chemical induction method (glass substrate with nerve growth factor (NGF) supplementation). Immunofluorescent staining for MAP2 in three groups after 7 days of culture and quantification of the body length of MAP2-positive cells are shown in Fig. S5. The MAP2-positive cell body was longer in the P3HT-NF group with photoelectrical stimulation ($187.4 \mu\text{m} \pm 50.8 \mu\text{m}$) than in other groups (glass group; $131.6 \mu\text{m} \pm 47.2 \mu\text{m}$, glass + NGF group; $173.4 \mu\text{m} \pm 30.2 \mu\text{m}$), but there was no statistical significance ($p > 0.05$) between P3HT-NF group and chemical induction group (glass + NGF). A qPCR result for MAP2 in hfNSCs in each group 7 days after culture showed that the expression of MAP2 was significantly enhanced ($p < 0.05$) in hfNSCs cultured on P3HT-NF substrate, compared to the cells on glass substrate (Fig. S5C). However, there was no significant difference ($p > 0.05$) in the gene expression of MAP2 in hfNSCs between P3HT-NF with photoelectrical stimulation group and chemical induction group (glass + NGF). Our results may indicate that optoelectrical stimulation of organic photovoltaics could remarkably increase neurogenesis of hfNSCs compared with the culture using conventional substrates, but the level of increment was similar to that of chemical induction.

hfNSCs differentiated on the P3HT-NF nanoweb with optoelectrical stimulation exhibited functional neuron-like electrophysiological features. Recently, it was demonstrated that photoelectrical stimulation of a P3HT-based photovoltaic blend increased the action potentials in hippocampal neurons [18, 55]. Thus, we examined the electrophysiological properties of hfNSCs differentiated on P3HT-NF substrates by

patch-clamping analysis. After 1 week of hfNSC culture on P3HT-NF with optoelectrical stimulation (1 Hz, 30 min twice per day), we observed the population of cells exhibiting voltage-dependent ionic current and action potentials (Fig. 5A and B). When the sodium channel antagonist TTX was used to treat the cells for 5 min, the action potential and sodium current completely disappeared, suggesting that the currents and spikes in hfNSCs on the P3HT-NF substrates were mainly mediated by sodium channels. Depolarization of hfNSCs on the P3HT-NF substrates by optoelectrical stimulation was also determined by examining the intracellular changes in calcium ion levels of hfNSCs upon light exposure for optoelectrical stimulation. When hfNSCs receiving optoelectrical stimulation for 7 days were treated with a Fluo-4 AM (Ca^{2+} -sensitive indicator) and then exposed to light stimulation, intracellular Ca^{2+} levels were increased in differentiated hfNSCs (Fig. S6), indicating ion channel activation and subsequent depolarization of hfNSCs. Overall, our data suggest that optoelectrical stimulation of photoactive P3HT substrates with nanotopographical NF structures significantly improved neuronal differentiation and functional maturation of human stem cells.

Although it is quite clear that optoelectrical stimulation of P3HT nanoweb could improve neurogenesis in human stem cells, we need to consider further studies related to maturation and other cellular behaviors. Actually, highly matured neurons exhibit repetitive firing and multiple peaks in electrophysiological evaluation [56, 57]. In this respect, the differentiated cells from hfNSCs on P3HT-NF substrates by light stimulation may not be fully matured since the cells showed only a single spike of action potential after depolarization (Fig. 5B). Our system based on P3HT nanostructured substrates with optoelectrical stimulation significantly improved neuronal differentiation of hfNSCs, but further studies would be required to facilitate functional maturation of differentiated cells similar to electrophysiological activity of mature neurons. Unlike conventional transfection methods to improve stem cell differentiation by transfecting specific genes to upregulate or silence targets, our approach based on optoelectrical stimulation of photoactive polymer materials is rather nonspecific since it is not clearly defined yet which factors are specifically regulated for stem cell differentiation by electrical stimulation. Therefore, further comprehensive experiments should be conducted to check whether other cellular behaviors and functions could be affected by optoelectrical stimulation.

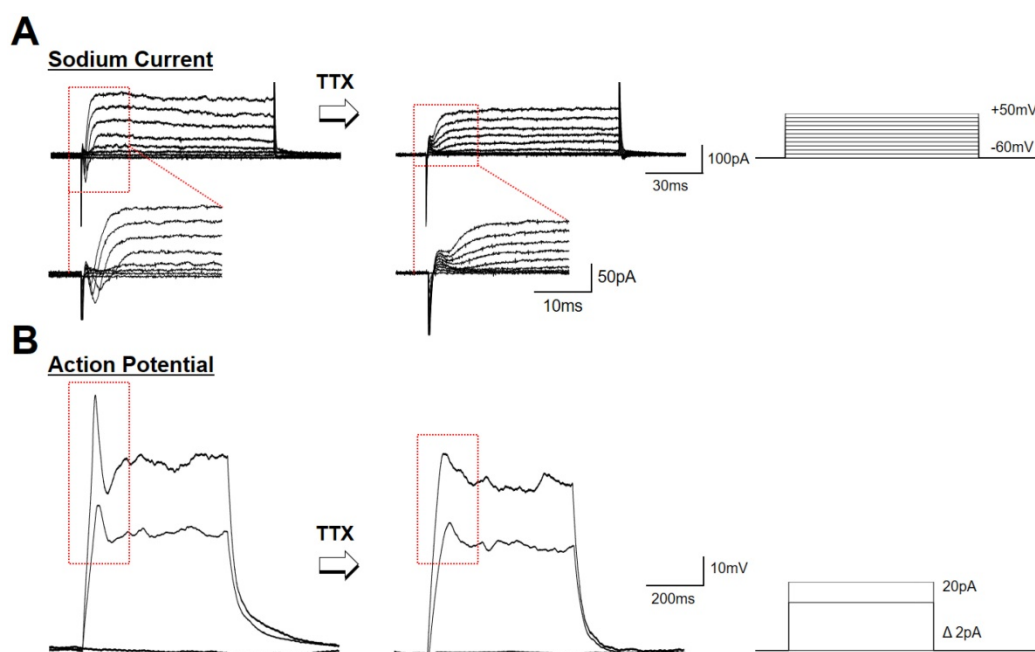


Figure 5. Electrophysiological evaluation of hfNSCs differentiated on P3HT-NF with optoelectrical stimulation for 7 days. Electrophysiological analysis using whole cell patch clamping was conducted to record sodium channel (A) currents and (B) action potential from differentiated hfNSCs on P3HT-NF with 539 nm light stimulation. The currents and action potential spikes disappeared after TTX treatment (sodium channel blocker).

One of the major limitations of the photo-induced electrical stimulation for *in vivo* applications is the intervention of light stimulation due to light absorption by tissue. Especially, it has been known that the light with 539 nm wavelength cannot penetrate deep into tissue due to significant light adsorption [58, 59]. Therefore, our strategy based on organic photovoltaics may provide implantable devices applicable for photoactivation and optogenetic manipulation in the tissues or organs accessible to external light stimuli. On the other hand, organic photovoltaic devices could be applied as culture platforms to produce functional, therapeutic cells exhibiting enhanced neurogenesis for the treatment of neurodegenerative diseases and neuronal disorders.

Optogenetic Modulation of hfNSC Neurogenesis on the P3HT Nanoweb

Finally, we investigated the utility of P3HT nanoweb substrates for optogenetic manipulation of hfNSC differentiation. Optogenetic approaches have been used to efficiently regulate the behaviors and functions of cells or tissues by using light-induced stimulation, particularly for neurons [27]. Thus, we hypothesized that our photoactive P3HT nanoweb responding to light exposure could be applied with optogenetic engineering of stem cells allowing for the simple manipulation of hfNSC differentiation by optical activation. ChR, a light-activatable ion channel, is one of the most important tools in

optogenetics for regulating neural activity via optical stimulation [27, 60]. Because P3HT substrates are stimulated by green light at 539 nm, we used color-tuned high efficiency ChRs based on chimeras of *Chlamydomonas reinhardtii* ChR-1 and *Volvox carteri* ChR-1 (C1V1), which can be activated by the same light source at 539 nm (Fig. 6A), for optogenetic manipulation of hfNSCs [60-63]. The engineered chimeric opsin variant, which contained point-mutated glutamic acid (E) to threonine (T) at 122 and 162 (C1V1 E122T/E162T; C1V1 ET-ET), was used to optically activate hfNSCs by light exposure at 539 nm [63]. To optogenetically modify hfNSCs, the cells were transfected with a C1V1 ET-ET-encoding plasmid through electroporation and then seeded onto FN-coated P3HT substrates under spontaneous differentiation medium condition without mitogens (bFGF and LIF). Two days after seeding, the hfNSCs were transfected again with the C1V1 ET-ET plasmids by using PBAE nanoparticles. Confocal microscopic observation confirmed successful transfection of the C1V1 plasmid with our protocol by detecting high expression of EYFP, which was inserted as a reporter in the plasmid construct, in the hfNSCs (Fig. 6B).

Optical manipulation of neuronal differentiation of hfNSCs was achieved with photoactive P3HT nanoweb substrates and optogenetically-engineered stem cells. The C1V1 ET-ET-transfected hfNSCs on the P3HT-NF substrates were cultured with pulsed optical stimulation by 539 nm LED light for 7 days (1 Hz, 30 min twice per day). qPCR analysis to

investigate the differentiation profiles of hfNSCs after 7 days in culture revealed that the C1V1 ET-ET-transfected hfNSCs on P3HT-NF stimulated with 539 nm light showed the most increased expression of neuronal markers (Tuj1 and MAP2) because of simultaneous optical stimulation of light-sensitive channel-expressing cells and photoactive substrates (Fig. 6C). Interestingly, the expression of Tuj1 and MAP2 was significantly upregulated in C1V1 ET-ET-transfected hfNSCs, even on glass in the presence of 539 nm light (Fig. 6C).

We determined the potential mechanisms of enhanced neurogenesis of C1V1 ET-ET-transfected

hfNSCs on photoactive P3HT nanoweb substrates by light stimulation. Previous studies reported that activation of C1V1 ET-ET by optical stimulation contributes to membrane depolarization and action potential generation in neurons with high levels of ChR expression [64, 65]. Membrane depolarization has been confirmed to play an important role in NSC differentiation and maturation [66-68]. Stroh *et al.* showed that when membrane depolarization in ChR-2 transfected embryonic stem cells was activated by optical stimulation, the stem cells tended to differentiate into functionally mature neurons exhibiting voltage-gated sodium currents, action

potentials, fast excitatory synaptic transmission, and expression of mature neuronal proteins and neuronal morphology [66]. Thus, we hypothesized that optoelectrical stimulation of photo-responsive nanoweb substrates and stem cells would promote neuronal differentiation by activating ion channels and membrane depolarization.

We investigated the expression of two types of ion channels in hfNSCs on the P3HT nanoweb with light stimulation. qPCR analysis after 7 days of culture revealed that the expression of SCN1 α was upregulated in C1V1 ET-ET-transfected hfNSCs cultured on P3HT-NF substrates with exposure to 539 nm green light compared to the cells cultured on glass or P3HT-NF substrates without light stimulation (Fig. 6D). In addition, the gene expression of CACNA1C was enhanced in hfNSCs grown on P3HT-NF substrates stimulated with 539 nm light (Fig. 6E). Our previous study reported that electrical stimulation created by a triboelectric nanogenerator activates voltage-gated calcium channels, increases calcium ion influx, and promotes

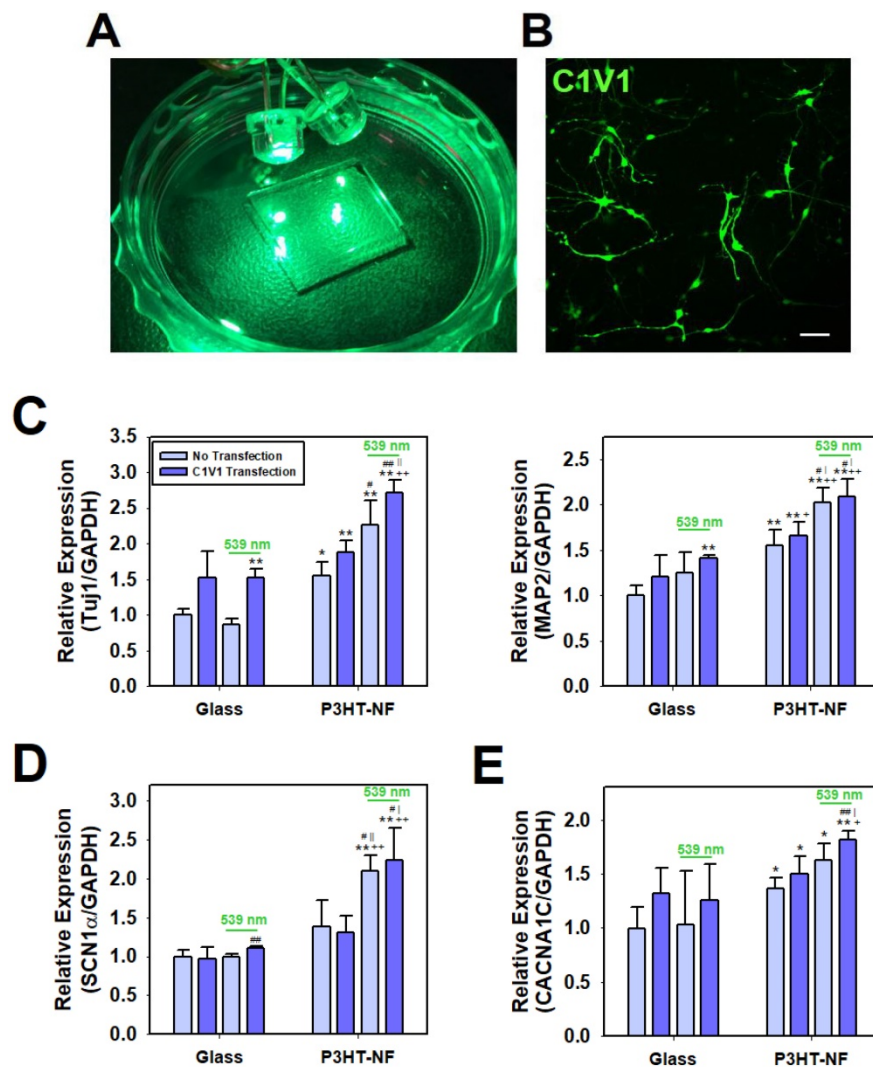


Figure 6. Optoelectrical stimulation for improving neuronal differentiation of optogenetically engineered hfNSCs on P3HT-NF nanoweb. (A) Green light (539 nm) was applied to hfNSCs transfected with C1V1 ET-ET/EYFP plasmids and P3HT substrates for 30 min twice per day (1 Hz). (B) Fluorescence microscopic observation to confirm C1V1 ET-ET/EYFP expression in hfNSCs 2 days after transfection, scale bar = 50 μ m. qPCR analysis to measure the gene expression of (C) neuronal markers (Tuj1 and MAP2), (D) voltage-gated sodium channel (SCN1 α), and (E) voltage-gated calcium channel (CACNA1C) in hfNSCs on each substrate after 7 days in culture ($n = 3$). The expression of target genes in each group was normalized to the level of hfNSCs cultured on glass without transfection and light stimulation (*; $p < 0.05$, **; $p < 0.01$, compared to glass group without C1V1 ET-ET transfection, +; $p < 0.05$, ++; $p < 0.01$, compared to glass group with C1V1 ET-ET transfection, #; $p < 0.05$, ##; $p < 0.01$, compared to P3HT-NF group without C1V1 ET-ET transfection, |; $p < 0.05$, ||; $p < 0.01$, compared to P3HT-NF group with C1V1 ET-ET transfection).

phosphorylation, eventually promoting neurogenesis [34]. Therefore, we predicted that simultaneous optoelectrical stimulation of P3HT-NF substrates and C1V1 ET-ET-transfected hfNSCs by 539 nm light would induce activation of ion channels (sodium and calcium channels), membrane depolarization, and subsequent signal transduction (e.g., ERK1/2) involved in neurogenesis, ultimately leading to the promotion of neuronal differentiation and functional maturation of hfNSCs. This is the first study to report the potential application of optoelectrical stimulation for enhanced neurogenesis of human stem cells based on photoactive polymer nanotopography.

Conclusions

In this study, we developed a photoactive polymer nanoweb with nanotopographical features to promote focal adhesion development and neuronal differentiation of hfNSCs. Photoactive nanoscale engineering of the interface between P3HT substrates and stem cells induced simultaneous activation of focal adhesion signals and electrical ion transport in hfNSCs, resulting in enhanced hfNSC neurogenesis. Indeed, a photocurrent generated by green light (539 nm) on the P3HT substrates with nanofibrillar structures (P3HT-NF) significantly promoted the neuronal differentiation and functional maturation of hfNSCs. The optoelectrical effect of P3HT-NF nanoweb on stem cell neurogenesis was further increased by nonviral optogenetic engineering of hfNSCs with the ChR plasmid, likely through the activation of voltage-gated ion channels for neurogenesis. This new strategy based on photoelectric systems with solar cell substrates and optogenetic tools provides a highly biocompatible and efficient method for enhancing stem cell neurogenesis. We suggest a proof of concept that optoelectrical technologies are potentially valuable engineering tools for stem cell therapy and regenerative medicine.

Abbreviations

P3HT: poly(3-hexylthiophene); hfNSCs: human fetal neural stem cells; ChR-1: channelrhodopsin-1; C1V1: *Chlamydomonas reinhardtii* ChR-1 and *Volvox carterii* ChR-1; NF: nanofibril; NR: nanorod; SEM: scanning electron microscopy; LED: light-emitting diode; FN: fibronectin; PL: photoluminescence; qPCR: quantitative real-time polymerase chain reaction; PBAE: poly(β -amino ester); PCMB: phenyl-C61-butyric acid methyl ester; rGO: reduced graphene oxide; TiO₂: titanium oxide; hMSCs: human mesenchymal stem cells; PEDOT: poly(3,4-ethylenedioxythiophene); NGF: nerve growth factor

Supplementary Material

Fig. S1–S6. <http://www.thno.org/v07p4591s1.pdf>

Acknowledgements

This work was supported by grants (2015R1A2A1A15053771, 2016M3C9A4921712, and 2017R1A2B3005994) from the National Research Foundation of Korea (NRF), the Ministry of Science, ICT and Future Planning (MSIP), Republic of Korea. This work was supported by the Institute for Basic Science (IBS-R026-D1).

Competing Interests

The authors have declared that no competing interest exists.

References

1. Yamada M, Tanemura K, Okada S, Iwanami A, Nakamura M, Mizuno H, et al. Electrical stimulation modulates fate determination of differentiating embryonic stem cells. *Stem Cells*. 2007; 25: 562-70.
2. Spitzer NC. Electrical activity in early neuronal development. *Nature*. 2006; 444: 707-12.
3. Pires F, Ferreira Q, Rodrigues CA, Morgado J, Ferreira FC. Neural stem cell differentiation by electrical stimulation using a cross-linked PEDOT substrate: expanding the use of biocompatible conjugated conductive polymers for neural tissue engineering. *Biochim Biophys Acta*. 2015; 1850: 1158-68.
4. Akhavan O, Ghaderi E, Shirazian SA, Rahighi R. Rolled graphene oxide foams as three-dimensional scaffolds for growth of neural fibers using electrical stimulation of stem cells. *Carbon*. 2016; 97: 71-77.
5. Thirivikraman G, Madras G, Basu B. Intermittent electrical stimuli for guidance of human mesenchymal stem cell lineage commitment towards neural-like cells on electroconductive substrates. *Biomaterials*. 2014; 35: 6219-35.
6. Seidlits SK, Lee JY, Schmidt CE. Nanostructured scaffolds for neural applications. *Nanomedicine*. 2008; 3: 183-99.
7. Stewart E, Kobayashi NR, Higgins MJ, Quigley AF, Jamali S, Moulton SE, et al. Electrical stimulation using conductive polymer polypyrrole promotes differentiation of human neural stem cells: a biocompatible platform for translational neural tissue engineering. *Tissue Eng Part C: Methods*. 2014; 21: 385-93.
8. Yang S, Jang L, Kim S, Yang J, Yang K, Cho SW, et al. Polypyrrole/alginate hybrid hydrogels: electrically conductive and soft biomaterials for human mesenchymal stem cell culture and potential neural tissue engineering applications. *Macromol Biosci*. 2016; 16: 1653-61.
9. Li N, Zhang Q, Gao S, Song Q, Huang R, Wang L, et al. Three-dimensional graphene foam as a biocompatible and conductive scaffold for neural stem cells. *Sci Rep*. 2013; 3: 1604.
10. Kim HW, Yang K, Jeong WJ, Choi SJ, Lee JS, Cho AN, et al. Photoactivation of noncovalently assembled peptide ligands on carbon nanotubes enables the dynamic regulation of stem cell differentiation. *ACS Appl Mater Interfaces*. 2016; 8: 26470-81.
11. Goenka S, Sant V, Sant S. Graphene-based nanomaterials for drug delivery and tissue engineering. *J Control Release*. 2014; 173: 75-88.
12. Xu B, Bai T, Sinclair A, Wang W, Wu Q, Gao F, et al. Directed neural stem cell differentiation on polyaniline-coated high strength hydrogels. *Mater Today Chem*. 2016; 1: 15-22.
13. Guo W, Zhang X, Yu X, Wang S, Qiu J, Tang W, et al. Self-powered electrical stimulation for enhancing neural differentiation of mesenchymal stem cells on graphene-poly (3, 4-ethylenedioxythiophene) hybrid microfibers. *ACS Nano*. 2016; 10: 5086-95.
14. Mohy-Ud-Din Z, Woo SH, Kim JH, Cho JH. Optoelectronic stimulation of the brain using carbon nanotubes. *Ann Biomed Eng*. 2010; 38: 3500-8.
15. Hsiao Y-S, Liao Y-H, Chen H-L, Chen P, Chen F-C. Organic photovoltaics and bioelectrodes providing electrical stimulation for PC12 cell differentiation and neurite outgrowth. *ACS Appl Mater Interfaces*. 2016; 8: 9275-84.
16. Wu J-L, Chen F-C, Chuang M-K, Tan K-S. Near-infrared laser-driven polymer photovoltaic devices and their biomedical applications. *Energy Environ Sci*. 2011; 4: 3374-8.
17. Jin G, Prabhakaran MP, Ramakrishna S. Photosensitive and biomimetic core-shell nanofibrous scaffolds as wound dressing. *Photochem Photobiol*. 2014; 90: 673-81.
18. Ghezzi D, Antognazza MR, Dal Maschio M, Lanzarini E, Benfenati F, Lanzani G. A hybrid biorganic interface for neuronal photoactivation. *Nat Commun*. 2011; 2: 166.

19. Oh JY, Shin M, Lee TI, Jang WS, Min Y, Myoung J-M, et al. Self-seeded growth of poly (3-hexylthiophene)(P3HT) nanofibrils by a cycle of cooling and heating in solutions. *Macromolecules*. 2012; 45: 7504-13.
20. Lee Y, Oh JY, Son SY, Park T, Jeong U. Effects of regioregularity and molecular weight on the growth of polythiophene nanofibrils and mixes of short and long nanofibrils to enhance the hole transport. *ACS Appl Mater Interfaces*. 2015; 7: 27694-702.
21. Ruan L, Zhang H, Luo H, Liu J, Tang F, Shi Y-K, et al. Designed amphiphilic peptide forms stable nanoweb, slowly releases encapsulated hydrophobic drug, and accelerates animal hemostasis. *Proc Natl Acad Sci USA*. 2009; 106: 5105-10.
22. Oh JY, Lee TI, Jang WS, Chae SS, Park JH, Lee HW, et al. Mass production of a 3D non-woven nanofabric with crystalline P3HT nanofibrils for organic solar cells. *Energy Environ Sci*. 2013; 6: 910-7.
23. Yang K, Jung K, Ko E, Kim J, Park KI, Kim J, et al. Nanotopographical manipulation of focal adhesion formation for enhanced differentiation of human neural stem cells. *ACS Appl Mater Interfaces*. 2013; 5: 10529-40.
24. Yang K, Jung H, Lee H-R, Lee JS, Kim SR, Song KY, et al. Multiscale, hierarchically patterned topography for directing human neural stem cells into functional neurons. *ACS Nano*. 2014; 8: 7809-22.
25. McNamara LE, McMurray RJ, Biggs MJ, Kantawong F, Oreffo RO, Dalby MJ. Nanotopographical control of stem cell differentiation. *J Tissue Eng*. 2010; 1: 120623.
26. Abagnale G, Steger M, Nguyen VH, Hersch N, Sechi A, Jousset S, et al. Surface topography enhances differentiation of mesenchymal stem cells towards osteogenic and adipogenic lineages. *Biomaterials*. 2015; 61: 316-26.
27. Boyden ES, Zhang F, Bamberg E, Nagel G, Deisseroth K. Millisecond-timescale, genetically targeted optical control of neural activity. *Nat Neurosci*. 2005; 8: 1263-8.
28. Yang HS, Lee B, Tsui JH, Macadangang J, Jang SY, Im SG, et al. Electroconductive nanopatterned substrates for enhanced myogenic differentiation and maturation. *Adv Healthc Mater*. 2016; 5: 137-45.
29. Yang K, Lee J, Lee JS, Kim D, Chang G-E, Seo J, et al. Graphene oxide hierarchical patterns for the derivation of electrophysiologically functional neuron-like cells from human neural stem cells. *ACS Appl Mater Interfaces*. 2016; 8: 17763-74.
30. Hong S, Yang K, Kang B, Lee C, Song IT, Byun E, et al. Hyaluronic acid catechol: a biopolymer exhibiting a pH-dependent adhesive or cohesive property for human neural stem cell engineering. *Adv Func Mater*. 2013; 23: 1774-80.
31. Yang K, Lee JS, Kim J, Lee YB, Shin H, Um SH, et al. Polydopamine-mediated surface modification of scaffold materials for human neural stem cell engineering. *Biomaterials*. 2012; 33: 6952-64.
32. Ko E, Yang K, Shin J, Cho SW. Polydopamine-assisted osteoinductive peptide immobilization of polymer scaffolds for enhanced bone regeneration by human adipose-derived stem cells. *Biomacromolecules*. 2013; 14: 3202-13.
33. Yang K, Park E, Lee JS, Kim IS, Hong K, Park KI, et al. Biodegradable nanotopography combined with neurotrophic signals enhances contact guidance and neuronal differentiation of human neural stem cells. *Macromol Biosci*. 2015; 15: 1348-56.
34. Jin Y, Seo J, Lee JS, Shin S, Park HJ, Min S, et al. Triboelectric nanogenerator accelerates highly efficient nonviral direct conversion and in vivo reprogramming of fibroblasts to functional neuronal cells. *Adv Mater*. 2016; 28: 7365-74.
35. Ko E, Yang K, Shin J, Cho SW. Polydopamine-assisted osteoinductive peptide immobilization of polymer scaffolds for enhanced bone regeneration by human adipose-derived stem cells. *Biomacromolecules*. 2013; 14: 3202-13.
36. Prabhakaran MP, Venugopal JR, Chyan TT, Hai LB, Chan CK, Lim AY, et al. Electrospun biocomposite nanofibrous scaffolds for neural tissue engineering. *Tissue Eng Part A*. 2008; 14: 1787-97.
37. Wu JL, Chen FC, Chang SH, Tan KS, Tuan HY. Upconversion effects on the performance of near-infrared laser-driven polymer photovoltaic devices. *Org Electronics*. 2012; 13: 2104-8.
38. Zhao L, Wang H, Huo K, Zhang X, Wang W, Zhang Y, et al. The osteogenic activity of strontium loaded titania nanotube arrays on titanium substrates. *Biomaterials*. 2013; 34: 19-29.
39. Luu TU, Gott SC, Woo BW, Rao MP, Liu WF. Micro-and nanopatterned topographical cues for regulating macrophage cell shape and phenotype. *ACS Appl Mater Interfaces*. 2015; 7: 28665-72.
40. McMurray RJ, Gadegaard N, Tsimbouri PM, Burgess KV, McNamara LE, Tare R, et al. Nanoscale surfaces for the long-term maintenance of mesenchymal stem cell phenotype and multipotency. *Nat Mater*. 2011; 10: 637-44.
41. Chan LY, Birch WR, Yim EK, Choo AB. Temporal application of topography to increase the rate of neural differentiation from human pluripotent stem cells. *Biomaterials*. 2013; 34: 382-92.
42. Yim EK, Darling EM, Kulangara K, Guilak F, Leong KW. Nanotopography-induced changes in focal adhesions, cytoskeletal organization, and mechanical properties of human mesenchymal stem cells. *Biomaterials*. 2010; 31: 1299-306.
43. Dingal PDP, Discher DE. Combining insoluble and soluble factors to steer stem cell fate. *Nat Mater*. 2014; 13: 532-7.
44. Pan Z, Yan C, Peng R, Zhao Y, He Y, Ding J. Control of cell nucleus shapes via micropillar patterns. *Biomaterials*. 2012; 33: 1730-5.
45. Seo CH, Jeong H, Furukawa KS, Suzuki Y, Ushida T. The switching of focal adhesion maturation sites and actin filament activation for MSCs by topography of well-defined micropatterned surfaces. *Biomaterials*. 2013; 34: 1764-71.
46. Robles E, Gomez TM. Focal adhesion kinase signaling at sites of integrin-mediated adhesion controls axon pathfinding. *Nat Neurosci*. 2006; 9: 1274-83.
47. Teo BKK, Wong ST, Lim CK, Kung TY, Yap CH, Ramagopal Y, et al. Nanotopography modulates mechanotransduction of stem cells and induces differentiation through focal adhesion kinase. *ACS Nano*. 2013; 7: 4785-98.
48. Turner CE. Paxillin and focal adhesion signalling. *Nat Cell Biol*. 2000; 2: E231-6.
49. Akhavan O, Ghaderi E. Flash photo stimulation of human neural stem cells on graphene/TiO₂ heterojunction for differentiation into neurons. *Nanoscale*. 2013; 5: 10316-26.
50. Suppes G, Ballard E, Holdcroft S. Aqueous Photocathode Activity of Regioregular Poly (3-Hexylthiophene). *Polymer Chem*. 2013; 4: 5345-50.
51. Lai LH, Gomulya W, Berghuis M, Protesescu L, Detz RJ, Reek JN, et al. Organic-Inorganic Hybrid Solution-Processed H₂-Evolving Photocathodes. *ACS Appl Mater Interfaces*. 2015; 7: 19083-90.
52. Gustafson MP, Clark N, Winther-Jensen B, MacFarlane DR. Organic photovoltaic structures as photo-active electrodes. *Electrochim Acta*. 2014; 140: 309-13.
53. Flynn KC. The Cytoskeleton and neurite initiation. *Bioarchitecture*. 2013; 3: 86-109.
54. Hsiao YS, Kuo CW, Chen P. Multifunctional graphene-PEDOT microelectrodes for on-chip manipulation of human mesenchymal stem cells. *Adv Func Mater*. 2013; 23: 4649-56.
55. Ghezzi D, Antognazza MR, Maccarone R, Bellani S, Lanzarini E, Martino N, et al. A polymer optoelectronic interface restores light sensitivity in blind rat retinas. *Nat Photonics*. 2013; 7: 400-6.
56. Song HJ, Stevens CF, Gage FH. Neural stem cells from adult hippocampus develop essential properties of functional CNS neurons. *Nat Neurosci*. 2002; 5: 438-45.
57. Moe MC, Varghese M, Danilov AI, Westerlund U, Ramm-Petersen J, Brundin L, et al. Multipotent progenitor cells from the adult human brain: neurophysiological differentiation to mature neurons. *Brain*. 2005; 128: 2189-99.
58. Ai X, Mu J, Xing B. Recent advances of light-mediated theranostics. *Theranostics*. 2016; 6: 2439-57.
59. Kobayashi H, Ogawa M, Alford R, Choyke PL, Urano Y. New strategies for fluorescent probe design in medical diagnostic imaging. *Chem reviews*. 2009; 110: 2620-40.
60. Tye KM, Deisseroth K. Optogenetic investigation of neural circuits underlying brain disease in animal models. *Nat Rev Neurosci*. 2012; 13: 251-66.
61. Yizhar O, Fenno LE, Davidson TJ, Mogri M, Deisseroth K. Optogenetics in neural systems. *Neuron*. 2011; 71: 9-34.
62. Klapoetke NC, Murata Y, Kim SS, Pulver SR, Birdsey-Benson A, Cho YK, et al. Independent optical excitation of distinct neural populations. *Nat Methods*. 2014; 11: 338-46.
63. Prigge M, Schneider F, Tsunoda SP, Shilyansky C, Wietek J, Deisseroth K, et al. Color-tuned channelrhodopsins for multiwavelength optogenetics. *J Biol Chem*. 2012; 287: 31804-12.
64. Packer AM, Roska B, Häusser M. Targeting neurons and photons for optogenetics. *Nat Neurosci*. 2013; 16: 805-15.
65. Prakash R, Yizhar O, Grewe B, Ramakrishnan C, Wang N, Goshen I, et al. Two-photon optogenetic toolbox for fast inhibition, excitation and bistable modulation. *Nat Methods*. 2012; 9: 1171-9.
66. Stroh A, Tsai HC, Wang LP, Zhang F, Kressel J, Aravanis A, et al. Tracking stem cell differentiation in the setting of automated optogenetic stimulation. *Stem Cells*. 2011; 29: 78-88.
67. Nakanishi S, Okazawa M. Membrane potential-regulated Ca²⁺ signalling in development and maturation of mammalian cerebellar granule cells. *J Physiol*. 2006; 575: 389-95.
68. Deisseroth K, Malenka RC. GABA excitation in the adult brain: a mechanism for excitation-neurogenesis coupling. *Neuron*. 2005; 47: 775-7.